Multi-Image Satellite SAR Interferometry: State of the Art and Future Trends

C. Colesanti[1,2], A. Ferretti[1,2], C. Prati[2], F. Rocca[2]

[1] Tele-Rilevamento Europa - T.R.E. S.r.l., Via V. Colonna, 7 –20149 Milano, Italy, Tel: ++39-02-4343121, Fax: ++39-02-43431230, e-mail: alessandro.ferretti@treuropa.com
[2] Dipartimento di Elettronica e Informazione, Politecnico di Milano, Piazza L. da Vinci, 32 -20133 Milano, Italy, Tel: ++39-02-23993451, Fax: ++39-02-23993413, e-mail: aferrett@elet.polimi.it

***Abstract* – In this paper we wish to review briefly the principles funding a recently developed approach, known as Permanent Scatterers (PS) technique and aimed at the joint exploitation of series of spaceborne interferometric SAR images for the retrieval of high precision elevation and ground deformation data on a sparse grid of privileged point-wise radar targets.**

I. INTRODUCTION

Conventional Synthetic Aperture Radar (SAR) interferometry (InSAR) deals with the pixel-by-pixel phase difference of two acquisitions, gathered at different times with slightly different looking angles [1], [2].
Spaceborne SAR interferometry has already proven a remarkable potential for two particular applications (of course among numerous others):

- The reconstruction of topographic digital elevation models (DEM) starting from interferometric pairs acquired from slightly different viewing angles [3]. (the core parameter summarising the different acquisition geometry is the so-called normal baseline).
- The detection of surface deformation phenomena (e.g. volcano in-/de-flation [4], co-seismic [5] and post-seismic [6] displacements along active faults as well as slope instability [7]) starting from pairs spanning a convenient time interval. It should be always kept in mind that only the projection of the occurring deformation along the sensor-target line of sight (LOS) can be appreciated in interferometric measurements.

Despite the theoretical capability of providing high precision elevation and deformation data, conventional InSAR has not yet become a fully operational tool.
Apart from cycle ambiguity problems, limitations are mainly due to temporal and geometrical decorrelation [8] (i.e. a single pixel reflectivity varying with time and/or with the acquisition geometry (it can be seen as complex fading)), and to atmospheric artefacts [9], [10].
Temporal decorrelation makes interferometric measurements unfeasible where the electromagnetic profiles and/or the positions of the scatterers change with time within the resolution cell (The use of short revisiting times can partially limit the effect, but only if the purpose is the DEM reconstruction).
Reflectivity variations as a function of the incidence angle (i.e. geometrical decorrelation) further limit the number of image pairs suitable for interferometric applications, unless this phenomenon is reduced due to the point-wise character of the target (e.g. a corner reflector).
In areas affected by either kind of decorrelation, reflectivity phase contributions are no longer compensated by generating the interferogram [8], and possible phase variations due to target motion cannot be highlighted [1].
Finally, atmospheric heterogeneity superimposes on each SAR image an atmospheric phase screen (APS) that can seriously compromise the precision of both topography and deformation estimates [1], [10]. Indeed, even considering areas slightly affected by decorrelation, it may be extremely difficult to discriminate displacement and topographic phase contributions from the atmospheric signature, at least using individual interferograms [1], [10].
In this paper we wish to illustrate how both drawbacks can often be overcome in a multi-image framework focusing the attention on privileged point-wise radar targets (hereafter called Permanent Scatterers), only slightly affected by decorrelation. PS mainly correspond to parts of man-made structures (in urban areas) and/or bare rock outcrops (especially in rural areas)
As described in the next section, the sparse grid of Permanent Scatterers can be exploited to estimate and remove the atmospheric signature.
The estimate of both exact elevation and deformation can, then, be faced on a pixel-by-pixel basis in a multi-image approach achieving precisions very close to the theoretical limits.

II. SAR PERMANENT SCATTERERS

All available images are focused and co-registered on the sampling grid of a unique master acquisition, which should be selected keeping as low as possible the dispersion of the normal baseline values. In order to make comparable the amplitude returns relative to different acquisitions, radiometric correction is carried out through power normalisation. Then, amplitude data are analysed on a pixel-by-pixel basis (without spatial averaging) computing the so-called amplitude stability index [11], [12], i.e. the ratio between the average amplitude return relative to each

individual pixel and its standard deviation. The amplitude stability index lets infer precious information about the expected phase stability of the scattering barycentre of each sampling cell. Simple thresholding (e.g. with a value of 2.5-3) on the amplitude stability index allows the identification of a sparse grid of Permanent Scatterers Candidates (PSC), points that are expected having a PS behaviour. (PSC are actually a small subset of the PS as a whole, since the phase stability of many PS cannot be inferred directly form the amplitude stability index).

Given N+1 ERS-SAR data, N differential interferogram can be generated with respect to the common master acquisition[1].

If a DEM (regardless whether interferometric or not) is available most of the topographic phase term is removed while generating the differential interferograms. Anyway, since in a further processing step residual topographic phase terms are estimated anyway, at this stage it is possible to compensate the interferograms for the flat Earth phase term only, isolating later the whole topographic phase contribution at individual PS [13].

As already mentioned, since Permanent Scatterers are not affected by decorrelation, all interferograms, regardless of their normal and temporal baseline can be involved in the PS processing. The phase of a generic pixel in interferogram *i* is:

$$\phi_i = \frac{4\pi}{\lambda} r_{Ti} + \alpha_i + n_i + \phi_{topo-res} \qquad (1)$$

where λ = 5.66 cm, r_{Ti} is the possible target motion (with respect to its position at the time of the master acquisition), α_i is the atmospheric phase contribution, n_i is the decorrelation noise $\phi_{topo\text{-}res}$ is the residual topographic phase contribution due to inaccuracy in the reference DEM (of course in case the PS analysis is being carried out assuming flat Earth, $\phi_{topo\text{-}res}$ identifies the elevation of the pixel at hand with respect to a reference ellipsoid).

Goal of the PS approach is the separation of these phase terms. The basic idea is to exploit their different spectral behaviour in a time-space[2]-acquisition geometry (i.e. normal baseline) multi-dimensional analysis [13]:

- r_{Ti} is correlated in time, can exhibit different degrees of spatial correlation depending on the phenomenon at hand and is uncorrelated with respect to the normal baseline.
- $\phi_{topo\text{-}res}$ is proportional (modulo 2π) to the normal baseline, is uncorrelated in time (and can be correlated or uncorrelated in space depending on the availability/characteristics of the reference DEM.
- α_i is strongly correlated in space and uncorrelated in time and normal baseline.

In practice, the first, rather cumbersome, step is the estimate of the APS. To this end we work on the PSC grid computing in each interferogram *i* the phase difference $\Delta\phi_i$ relative to pairs of PSC within a certain maximum distance (e.g. 2 km).

In fact, since APS is strongly correlated in space, the differential atmospheric phase contributions relative to close PSC will be extremely low (for points less than 1 km apart $\sigma_{\Delta\alpha}^2$ is usually lower than 0.1 rad^2 [14]).

The phase difference relative to close PSC is, therefore, only slightly affected by APS.

Moreover, if both PSC, effectively exhibit PS behaviour (i.e. are not affected by decorrelation), n_i and, consequently, Δn_i will show a very low variance as well.

Assuming the target motion is uniform in time (i. e. constant rate deformation), the first term in (1) can be written as $(4\pi/\lambda)vT_i$, where v is the average deformation rate along the ERS Line of Sight (LOS) and T_i is the temporal baseline with respect to the master acquisition.

For a couple of PSC (1,2), respectively in positions (n_1,m_1) and (n_2,m_2), the phase difference in each interferogram *i* is:

$$\Delta\phi_{1,2,i} = \frac{4\pi}{\lambda}\Delta v_{1,2} T_i + K_\varepsilon \Delta\varepsilon_{1,2} B_{n,i} + w_{1,2,i} \qquad (2)$$

where $\Delta v_{1,2}$ and $\Delta\varepsilon_{1,2}$ are the differential LOS velocity and the differential DEM error relative to the PS couple at hand. $B_{n,i}$ is the normal baseline relative to interferogram *i* and $w_{1,2,i}$ is the residual phase term, gathering decorrelation noise, differential APS and possible time non-uniform deformation.

Since N differential interferograms are available, for each couple of PSC we are facing N equations in the unknowns $\Delta v_{1,2}$ and $\Delta\varepsilon_{1,2}$. Unfortunately the phase values $\Delta\phi_{1,2,i}$ are wrapped, and, therefore, the system is non-linear. In fact, even if no deformation is occurring, the differential residual topographic phase will often exceed one phase cycle in large baseline interferograms (e. g. for a 1200 m baseline interferogram the height of ambiguity [2] is around 7.5 m).

The unknowns can be estimated as the position $(\Delta v_{1,2},\Delta\varepsilon_{1,2})$ of the peak in the periodogram of the complex signal $e^{j\Delta\phi(1,2,i)}$ (for a regularly $(T_i,B_{n,i})$ sampled signal $e^{j\Delta\phi(1,2,i)}$ the periodogram based estimate turns out being Maximum Likelihood [15]. In our case $e^{j\Delta\phi(1,2,i)}$ is irregularly sampled).

Of course this is feasible only as long as $w_{1,2,i}$ is low enough.

As soon as $\Delta v_{1,2}$ and $\Delta\varepsilon_{1,2}$ are available, the phase differences $\Delta\phi_i$ can be unwrapped correctly (of course assuming $|w_{1,2,i}|<\pi$). Integrating the unwrapped phase differences relative to every couple of PSC, each interferogram can be unwrapped in correspondence of the

[1] In this paper we will refer always to ESA ERS data sets.

[2] As implicitly specified later, the space dimension is the distance between PS evaluated in range-azimuth image space.

PSC mask (sparse grid phase unwrapping, in partial analogy with what discussed in [16]).
Moreover $\Delta v_{1,2}$ and $\Delta \varepsilon_{1,2}$ can be integrated as well (assuming $v = v_0$ and $\varepsilon = \varepsilon_0$ for a reference PSC, possibly on the basis of a priori information), obtaining v and ε.
The unwrapped atmospheric phase contribution relative to each PSC can be obtained as the difference:

$$\left[\alpha_i\right]_{uw} = \left[\phi_i\right]_{uw} - \frac{4\pi}{\lambda} v T_i - K_\varepsilon \varepsilon B_{n,i} \qquad (3)$$

Of course, possible time non-uniform deformation phenomena are, so far, wrongly interpreted as atmospheric artefacts. As already mentioned, the two phase contributions exhibit a different behaviour in time: APS is uncorrelated whereas non-linear motion (NLM) is usually strongly correlated.
Assuming a time decaying exponential correlation for NLM, corrected with a 1 year periodic term (for possible NLM seasonal effects), APS and time non-uniform deformation can be separated at PSC, through Wiener filtering along time dimension (taking account of the irregular sampling in time, induced by missing ERS acquisitions).
Due to the high spatial correlation of APS, even a sparse grid of PSC enables to retrieve the atmospheric components on the whole of the imaged area, provided that the PS density is larger than 3-4 PS/km^2. Kriging interpolation [17] allows optimum filtering and re-sampling of APS on the regular SAR grid of the ERS differential interferograms (filtering is extremely precious to reduce the impact of possible outliers and, again, to enhance separation of spatially uncorrelated time non-uniform deformation phenomena from the estimated APS (e.g. single structure instability affecting individual PSC)).
Differential interferograms are compensated for the retrieved APS (actually APS + orbit indetermination phase term, as we shall see later), and the same v,ε estimation step, previously carried out only at couples of PSC on the corresponding phase differences, can now be performed working on APS corrected interferograms on a pixel-by-pixel basis, identifying all Permanent Scatterers.
At this stage more complex models for surface deformation can easily be introduced [13].
Of course, a sufficient number of images should be available (even tough there are not rigid limits, a reasonable figure is 20 [13]), in order to properly identify PSC and correctly estimate $\Delta v_{1,2}$ and $\Delta \varepsilon_{1,2}$.

III. A FEW OBSERVATIONS

Having described briefly the PS scheme a few observations are in order:

- Even though precise state vectors are usually available for ERS satellites [18], the impact of orbit indeterminations on the interferograms cannot be neglected. This latter phase term can usually be modelled well with a second order polynomial within a single interferogram [10] and, of course, is uncorrelated in time. Its spectral behaviour is therefore similar to the one of APS. As a matter of fact the estimated APS is actually the sum of two contributions: atmospheric effects and orbital fringes due to baseline errors [12], [13].
- The elevation estimate carried out at PSC couples can be seen as a sparse grid version of the well known multi-baseline phase unwrapping approach ([19], [20]), field of ongoing research both for topography reconstruction [21], [22] and layover solution issues [22], [23] (of course, in the framework of a PS analysis, long time span interferograms are involved as well, and, as already mentioned, elevation and LOS velocity of individual targets are estimated jointly). The core idea of a multi-baseline approach is the joint exploitation of more interferograms with different normal baseline values in order to increase reliability and precision of the elevation estimate. Very intuitively, this allows one to couple the advantageous high sensitivity to topography of large baseline interferograms with the reduced risk of introducing unwrapping errors of lower baseline interferometric pairs. As already mentioned, working only on privileged radar targets, not affected by decorrelation, allows one to exploit optimally the multi-baseline principle involving even interferograms with baselines larger than the critical one (about 1100 m for ERS data). This translates immediately in an extraordinary sub-metre precision (σ_ε<1 m) of the single PS elevation estimates [11], [13].
- The precision in vertical PS positioning turns out being extremely important since it translates directly in a high geocoding precision that (provided that a systematic offset can be determined and compensated for) allows one to map the Permanent Scatterers on the corresponding structures.

We get following simple expression for the positioning uncertainty along ground range σ_{gr}:

$$\sigma_{gr} = \sqrt{\frac{\sigma_\varepsilon^2}{(\tan\theta)^2} + \frac{\sigma_{sr-pos}^2}{(\sin\theta)^2}} \qquad (\approx 3.75\ m) \qquad (4)$$

where θ is the local incidence angle ($\theta \approx 23°$ for flat terrain in the centre of an ERS scene) and $\sigma_{sr\text{-}pos}$ is the slant range position uncertainty. The indicative numerical figure of 3.75 m was obtained with σ_ε=1 m and assuming the PS position being uniformly distributed within the slant range sampling interval (a range oversampling factor of 2 has been taken into account: $\sigma^2_{sr\text{-}pos}=(\Delta_{sr}/2)^2/12$, where Δ_{sr} is the original slant-range sampling step (7.9 m for ERS)).

- Final results of the multi-interferogram Permanent Scatterers approach are [11], [12], [13][3]:

[3] Both correctness and precision figures for PS results have been validated in the comparison with optical leveling records, solutions from permanent GPS stations, and creepmeters along seismic faults [13].

I. Map of the PS identified in the image and their co-ordinates: latitude, longitude and precise elevation;
II. Average LOS deformation rate of every PS (precision between 0.1 and 0.5 mm/yr., depending on the number of available interferograms and on the phase stability of each single PS, [13]);
III. Displacement time series showing the relative (i.e. with respect to a selected unique reference image) LOS position of PS in correspondence of each SAR acquisition. Time series identify, therefore, the LOS motion component of PS as a function of time (precision on single measurements usually ranging from 1 to 3 mm, [13]).

As in all differential interferometry applications, results are computed with respect to a reference point of known elevation and motion.

IV. RESULTS

We wish now to illustrate very briefly a few significant results obtained by means of the Permanent Scatterers technique on two test sites Milano (Italy) and Triesenberg (Füstentum Liechtenstein).

84 ERS-1/2 SAR images covering the time span May 1992 – October 2002 (Track 208, Frame 2691, descending mode) have been involved in the PS analysis carried out on Milano.

The first purpose is to demonstrate operationally that PS can be mapped on the corresponding structures and that, therefore, the PS technique really allows a single building monitoring.

To this end we simply superimposed PS results as a point-vector data layer to further geographic layers in a GIS (Geographic Information System) environment (in particular to the urban texture and the street graph layers), see Figure 1.

A further issue is to prove how, despite the failures occurred on ERS-2 gyros (7 February 2000 and, later, 17 January 2001), ERS-2 data acquired in Mono-Gyro mode (MGM) and Zero-Gyro mode (ZGM) [25] can still be exploited successfully in the framework of a PS analysis[4] (see Figure 2).

We present also some results relative to the PS investigation of the Triesenberg-Triesen landslide located in the Swiss Alps. 38 descending mode ERS data covering the time span August 1992 – August 2001 were exploited. The unstable area is located on the Eastern slopes of the Rhine Valley, in Liechtenstein, approximately 30-40 km North of the Swiss town of Chur. The landslide slope faces approximately west, which makes the exploitation of descending mode data ideal for interferometric purposes.

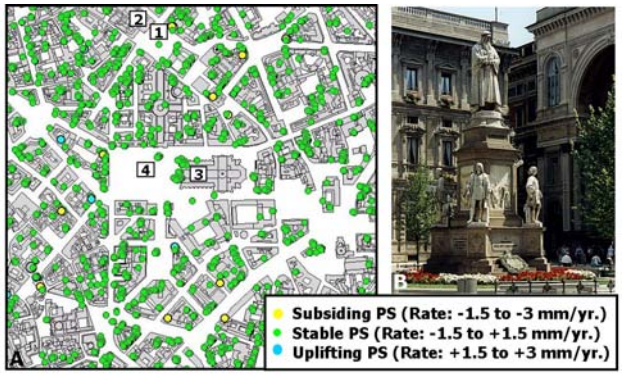

Figure 1: A. Permanent Scatterers (Milano) mapped on the corresponding structures in GIS environment (GIS data: [24]). The PS marked (1) corresponds to the monument to Leonardo da Vinci in the centre of "Piazza della Scala" (photo in B), the one marked (4) to the entrance to the underground in "Piazza del Duomo". No PS were identified on apse and transept of the Cathedral (3) as well as on the theatre "alla Scala" because of restoration interventions lasted years.

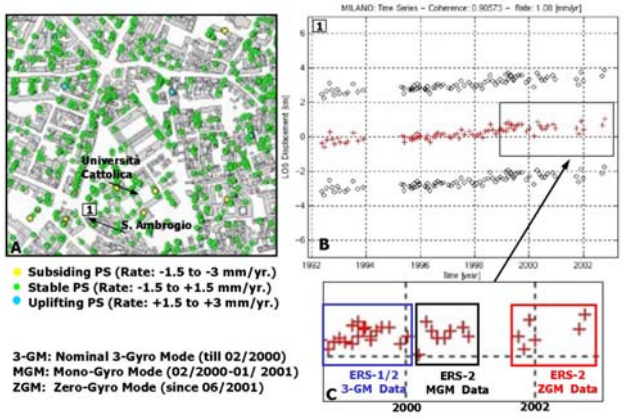

Figure 2: A. PS in GIS environment (Milano). B. Time series relative to a PS on the St. Ambrosius Basilica (±λ/2 solutions are represented as well). C. Zoom highlighting MGM and ZGM data (the slightly increased dispersion of ZGM data is probably due to the finite extension of the PS in azimuth direction coupled with larger Doppler centroid values).

The unstable area includes the town of Triesen (located near the bottom of the valley), and of Trisenberg (located more upslope). The Triesenberg-Triesen landslide has an area of 4.2 km^2 and a volume of about 500 million cubic meters. The origins of the landslide may date back to the retreat of the Rhine Glacier occurred about 12,000 years ago [26].

The application of the PS technique resulted in the identification of around 7500 PS in the 16x16 km^2 test site

[4] In case of distributed scattering the attitude instability is an additional source of decorrelation (analogous to geometrical decorrelation), whereas for point-wise scatterers an additional deterministic phase contribution is introduced and can be estimated and removed. The discussion of the methodology used to this end is well beyond the purposes of this paper.

area (average density of 30 PS/km^2). The area analysed is approximately in the centre of a full ERS scene (Track: 480, Frame: 2655, Mode: descending).

As already mentioned, the area affected by the landslide covers the territory of the municipalities of Triesenberg and Triesen, and nearly reaches the bottom of the valley (Figure 3). The boundaries of the deforming area can be identified very clearly by following a sharp velocity gradient existing between the PS located within the landslide body and stable points present in the surrounding area (Figure 3).

Around 450 PS were identified within the area affected by most significant deformation ($|v_{LOS}|$>2mm/yr.) and its surroundings (approximately 1.7x2.2 km^2).

The local PS density amounts, therefore, to around 120 PS/km^2. LOS deformation rates vary from -2 to -20 mm/yr.

The graphs in Figure 3 (B and C) show also the LOS displacement time series of two PS (points 1., 2.) located in the Triesenberg area. The evolution of PS 1 is not time-uniform, highlighting three quiescent periods, respectively in late 1992 and in the first months of 1995 and 1996. The standard deviation on each measurement can be computed [13] and turns out being slightly lower than 2 mm. The time series relative to PS 2, situated at few hundred meters distance from PS1, shows a much slower displacement and is slightly noisier ($\sigma \approx 2.2$mm).

A closer examination of Figure 3 allows one to appreciate several differential dynamics within the main landslide body clearly highlighted by the sub-millimetric precision of PS velocity estimates.

Finally, a densely vegetated valley slope area to the south of the main landslide contains two more PS, indicating the presence of ongoing deformations. Although neither ground truth nor in situ measurements are available, the examination of aerial photos suggests that these PS could be located on what appears to be an old landslide [27]. This case illustrates the usefulness of the PS technique for the recognition of previously unknown, potential landslide hazard areas.

V. CONCLUSIONS AND RESEARCH ISSUES

The PS approach is a fully operational tool for high precision wide area ground deformation monitoring. Among the main advantageous aspects: the capability of providing single pixel deformation data (and, therefore, the of exploiting individual phase stable targets in incoherent areas), the millimetric precision, the possibility to map directly the deformation data on the corresponding structures (due to the precise elevation estimate), the high density of measurement points (in urban areas sometimes even more than 500 PS/km^2) and, finally, the possibility of investigating past deformation phenomena, exploiting the ESA ERS archive.

Despite the full operational capability, a lot of research issues are open and are currently being faced:

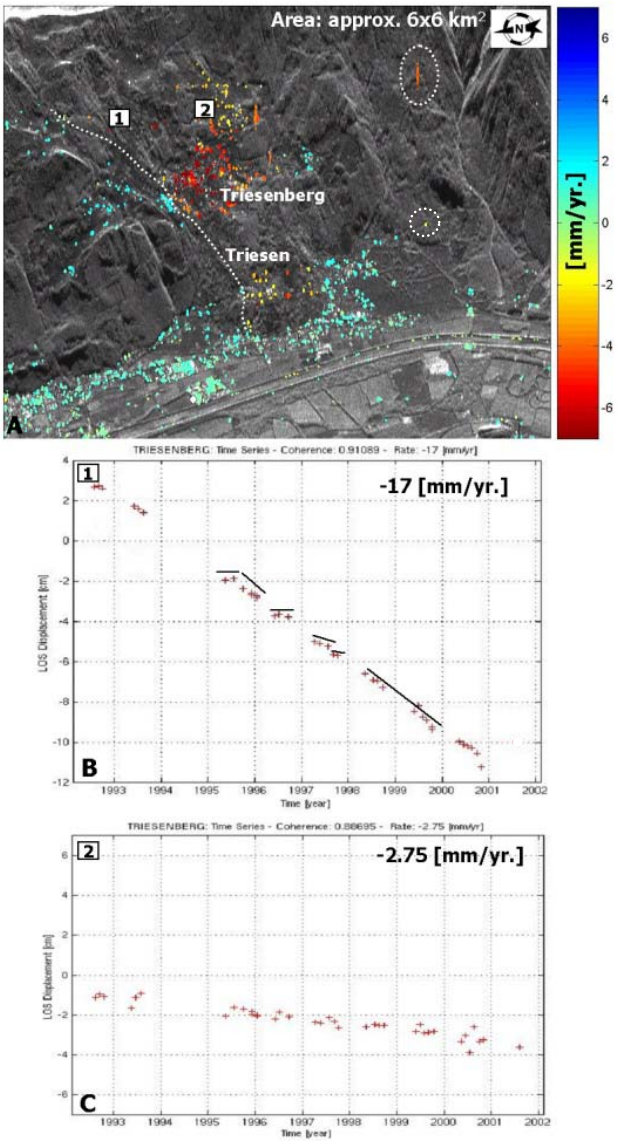

Figure 3: A. PS average LOS displacement rate superimposed on a multi-image reflectivity map. Velocity values are saturated between ±7 mm/yr for visualization purposes only. The boundaries of the sliding area as well as internal differential dynamics can be appreciated immediately. B.-C. LOS displacement time series of individual PS.

- Series of RADARSAT and JERS data start being analysed by means of the PS approach. The most interesting issue to be evaluated is the impact of different operating frequencies (C-band for ERS and RADARSAT vs. L-band for JERS) and polarisations (VV for ERS vs. HH for RADARSAT and JERS), as well as incidence angles and resolutions (in particular fine beam RADARSAT data) on the PS population.

- Despite the 30 MHz frequency shift, it seems theoretically possible (and is currently being attempted) to perform on the PS a coherent ERS-ENVISAT time series stitching (i.e. to exploit ERS-ENVISAT interferograms).

ACKNOWLEDGMENTS

The authors wish to thank ESA-ESRIN for providing the ERS data set relative to Milano under contracts no. 13557/99/I-DC and 16564/02/I-LG. Ing. R. Ratti cooperated intensively in carrying out the PS analysis on the Triesenberg-Triesen landslide that was performed in the framework of the EC project MUSCL (Monitoring Urban Subsidence Cavities and Landslides by means of remote sensing, 5th RTD Framework of the European Commission, EVG1-CT-1999-0008).
We acknowledge also Dr. S. Liener (GEOTEST A.G., Switzerland) and Dr. J. Wasowski (CNR-CERSIT, Bari, Italy) as well as the whole TRE staff that developed and engineered the PS software.

REFERENCES

[1] D. Massonnet, K. L. Feigl, "Radar Interferometry and its Application to Changes in the Earth's Surface", Rev. of Geophysics, 36, 1998.
[2] P. A. Rosen, S. Hensley, I. R. Joughin, F. K. Li, S. N. Madsen, E. Rodriguez, R. M. Goldstein, "Synthetic Aperture Radar Interferometry", Proc. of the IEEE, Vol. 88, No. 3, 2000.
[3] H. A. Zebker, R. M. Goldstein, "Topographic Mapping from Interferometric Synthetic Aperture Radar Observations", Journal of Geoph. Res., Vol. 91, 1986.
[4] D. Massonnet, P. Briole, A. Arnaud, "Deflation of Mount Etna monitored by Spaceborne Radar Interferometry", Nature, 375, 1995.
[5] D. Massonnet, M. Rossi, C. Carmona, F. Adragna, G. Peltzer, K. Feigl, T. Rabaute, "The Displacement Field of the Landers Earthquake Mapped by Radar Interferometry", Nature, 364**,** 1993.
[6] D. Massonnet, K. Feigl, M. Rossi, F. Adragna, "Radar Interferometric Mapping of Deformation in the Year after the Landers Earthquake", Nature, 369, 1994.
[7] B. Fruneau, J. Achache, C. Delacourt, "Observation and Modeling of the Saint-Etienne-de-Tinée Landslide Using SAR Interferometry", Tectonophysics, 265, 1995
[8] H. A. Zebker, J. Villasenor, "Decorrelation in Interferometric Radar Echoes", IEEE Trans. on Geosc. and Rem. Sens., Vol. 30, No. 5, 1992
[9] H. A. Zebker, P. A. Rosen, S. Hensley, "Atmospheric Effects in Interferometric Synthetic Aperture Radar Surface Deformation and Topographic Maps", Journal of Geoph. Res., Vol. 102, 1997.
[10] R. F. Hanssen, "Radar Interferometry. Data Interpretation and Error Analysis", Dordrecht, Kluwer Academic Publishers, 2001
[11] A. Ferretti, C. Prati, F. Rocca, "Permanent Scatterers in SAR Interferometry", IEEE Trans. on Geosc. and Rem. Sens., Vol. 39, No. 1, 2001.
[12] A. Ferretti, C. Prati, F. Rocca, "Non-linear subsidence rate estimation using permanent scatterers in Differential SAR Interferometry", IEEE Trans. on Geosc. and Rem. Sens, Vol. 38, No. 5, 2000.
[13] C. Colesanti, A. Ferretti, F. Novali, C. Prati, F. Rocca, "SAR Monitoring of Progressive and Seasonal Ground Deformation Using the Permanent Scatterers Technique", IEEE Trans. on Geosc. and Rem. Sens., in press.
[14] S. Williams, Y. Bock, P. Pang, "Integrated Satellite Interferometry: Tropospheric Noise, GPS Estimates and Implications for Interferometric Synthetic Aperture Radar Products", Journal of Geoph. Res., Vol. 103, 1998.
[15] D. C. Rife, R. R. Boorstyn, "Single-tone parameter estimation from discrete-time observations", IEEE Trans. on Inf. Theory, Vol. IT-20, 1974.
[16] M. Costantini, P.A. Rosen, "A generalized phase unwrapping approach for sparse data", Proc. of IEEE IGARSS 1999, Hamburg, 1999
[17] H. Wackernagel, Multivariate Geostatistics, IInd Edition, Springer Verlag, Berlin, 1998.
[18] R. Sharroo, P. Visser, "Precise Orbit Determination and Gravity Field Improvement for the ERS Satellites, Journal of Geoph. Res., Vol. 103, 1998.
[19] A. Ferretti, A. Monti Guarnieri, C. Prati, F. Rocca, "Multi Baseline Interferometric Techniques and Applications", Proc. of FRINGE 1996, Zurich, 1996.
http://www.geo.unizh.ch/rsl/fringe96/papers/ferretti-et-al/
[20] P. Lombardo, F. Lombardini, "Multi-baseline SAR interferometry for terrain slope adaptivity" Proc. of the IEEE Radar Conference, Syracuse (NY), 1997.
[21] A. Ferretti, C. Prati, F. Rocca, "Multibaseline Phase Unwrapping for InSAR Topography Estimation", Il Nuovo Cimento, Vol. 124, No. 1, 2001
[22] F. Gini, F. Lombardini, "Multilook APES for multibaseline SAR interferometry", IEEE Trans. on Signal Proc., Vol. 50, No.7, 2002.
[23] F, Gini, F. Lombardini, M. Montanari, "Layover solution in multibaseline SAR interferometry", IEEE Trans. on Aerosp. and Electonic Syst., Vol. 38, No. 4, 2002.
[24] Urban Explorer, produced by Assimpredil (http://www.assimpredil.ance.it) in cooperation with the Municipality of Milano, (http://www.comune.milano.it).
[25] ESA Earth Observation Product Control Service, http://earth.esa.int/pcs/ers/sar/doppler/
[26] S. Liener, written communication, 2002.
[27] J. Wasowski, written communication, 2002.